Transport Through a Clay Barrier with the Contaminant Concentration Dependent Permeability

MARIUSZ KACZMAREK[1,*], TOMASZ HUECKEL[1], VIKAS CHAWLA[1,**] and
PIERLUIGI IMPERIALI[2]
[1]*Duke University, Durham, NC 27708-0287, U.S.A.*
[2]*ISMES, via Pastrengo, 9, 24068 Bergamo, Italy*

Abstract. Transport of contaminants through clays is characterized by a very low dispersivity, but depends on the sensitivity of its intrinsic permeability to the contaminant's concentration. An additional constitutive relationship for a variable intrinsic permeability is thus adopted leading to a coupled system of equations for diffusive–advective transport in multicomponent liquid. A one-dimensional transport problem is solved using finite difference and Newton–Raphson procedure for nonlinear algebraic equations. The results indicate that although diffusion contributes to an increase of transport with respect to pure advection, the flux ultimately depends on end boundary conditions for concentration which, if low, may actually slow down the evolution of concentration and thus of permeability. Indeed, the advective component of flux may still remain secondary if the end portion of the layer remains unaffected by high concentrations. With no constraints on concentration at the bottom (zero concentration gradient boundary condition) and high concentration applied at the top, a significant shortening of the breakthrough time occurs.

Key words: variable permeability, contaminant transport, advection/diffusion, clays, organics, finite difference.

1. Introduction

Soil liners are major components of containment barriers of waste landfill. They determine an effectiveness of the barriers against the transport of liquid contaminants into groundwater and, consequently, the safety of the landfill operation. One of the important tools used in the design of landfill liners is the numerical simulation of the contaminant transport process. In addition to the prediction of the flux of the contaminant, it is used to assess the role of different physico-chemical mechanisms influencing the transport in the evolution of contamination. Although, the legislative requirements for liner materials impose limits on hydraulic conductivity only (its maximum value is usually limited to 10^{-6} or 10^{-7} cm/s), at least four mechanisms: advection, diffusion, dispersion, and sorption control the transport of contaminants through the low permeability barriers (see, e.g., [21, 22, 24]). Moreover, it is experimentally well documented that the intrinsic permeability of clayey soils, which are

---

⋆ Present address: Department of Environmental Mechanics, College of Education, Bydgoszcz, Chodkiewicza 30, 85-064 Bydgoszcz, Poland.
⋆⋆ Present address: Hibbit, Karlsson and Sorensen, 1080 Main St., Pawtuckett, RI 02860, U.S.A.

widely used as liner materials, may be substantially altered by some concentrated organic contaminants, see, e.g., [9, 16]. Microscopic mechanisms responsible for the changes are of physico-chemical and/or purely chemical nature. Redistribution of the pore space driven by dehydration of clay fraction, and rearrangement of clay particles (flocculation, peptization, and micro-migration) together with chemical reactions between contaminants and clay mineral, such as dissolution of the solids are believed to be the most important causes of the permeability evolution. In the case of liners beneath domestic landfills, the sensitivity of the liner material to organic contaminants is especially important. A number of experimental studies have shown that intrinsic permeability increase in such a case may range few orders of magnitudes. Since concentration may change due to both advection and diffusion, even in the materials having a very low permeability initially, advection may increase due to diffusive transport resulting in an eventual massive flow. Density and viscosity of contaminant–water mixture are also functions of the concentration of contaminant [27]. Finally, concentration and pressure at liner boundaries change due to variability of environmental conditions.

The above factors require that the transport processes in liners be approached as coupled phenomena. Existing models of coupled transport phenomena in saturated porous materials deal with the dependence of mass fluxes on gradients of pore pressure, temperature, and concentration of chemicals (e.g. [15]). In the proposed formulation, the dispersive transport depends on advection through mechanical dispersion, while through the concentration sensitive permeability the advective transport depends on diffusion. As a result, a solution of a coupled nonlinear system of equations is required.

The role of the chemically induced changes of porosity through dissolution or precipitations of minerals, and as a result of permeability on spatial and temporal evolution of the transport was studied for rock materials, e.g. by Steefel and Lasaga [25], and Carnahan [5]. In these models the central role is played by porosity changes. However, this is not the case of low permeability clayey materials permeated by concentrated organics, which do not include significant changes in porosity, as amply demonstrated by Acar *et al.* [1] and Fernandez and Quigley [8, 9].

The purpose of this paper is to study advective/diffusive/dispersive transport of a contaminant through the chemically sensitive clay layer with intrinsic permeability dependent on the concentration, which affects the tiny, bottle neck elements of flow channels, without much effect on the overall porosity [14]. Thus, the solid skeleton is assumed as undeformable, i.e. with stress and contamination insensitive porosity. The liquid phase is assumed to be a mixture of strongly interacting components [26]. This implies that a single balance of linear momentum is considered for the whole liquid phase, while for its components separate balances for mass conservation only are taken into account. Chemical reactions between liquid components and chemical interactions of liquid with solid are disregarded. A central point of this approach are the changes of permeability induced by the chemical dehydration of clay fraction. The process of transport of a contaminant is assumed to be isothermal and slow enough

to neglect inertial effects. The study is limited to a one-dimensional implementation of the coupled model. Numerical simulation of the process is performed using finite-difference formulation based on backward Euler upwind differencing scheme of the coupled system of governing equations. The Newton–Raphson algorithm is used for solution of the resultant system of non-linear algebraic equations. Although the presence of concentrated organics in the landfill leachate may be viewed as a limiting case, it may occur locally in sufficient quantities to cause a critical situation. Also, industrial impoundments may contain significant amounts of concentrated organics. Concentrated dioxane is taken as an example of contaminant in this paper using the data on its effect on Sarnia clay obtained by Fernandez and Quigley [8–10].

2. Description of the Model

2.1. BALANCE EQUATIONS

The principle of conservation of mass for the whole mass of liquid implies that the relation between the intrinsic density of liquid, ρ, and the mass average advective velocity of the liquid phase $\mathbf{v}$, be expressed as follows:

$$\frac{\partial(n\rho)}{\partial t} + \nabla \cdot (n\rho\mathbf{v}) = 0, \tag{1}$$

where n is an effective porosity of the liner material. Since most of the soil liner materials contain clay fraction, a significant amount of water in the materials is adsorbed on the surface of clay particles. As a result, the flow of liquid and advective component of transport are limited to the pore space which is filled with mobile (nonadsorbed) liquid. The effective porosity, n, represents the volume fraction of the mobile liquid. The importance of the effective porosity in modeling of transport phenomena results from the fact that it relates the velocity of advective transport, $\mathbf{v}$, to discharge velocity, $\mathbf{q}$, i.e. $\mathbf{q} = n\mathbf{v}$, which is a basic measured quantity for flow through porous media.

If the liquid saturating the porous medium is a mixture of N chemically inert components, then $(N-1)$ independent mass balances for components, should be satisfied [11], i.e.

$$\frac{\partial(n\rho^i)}{\partial t} + \nabla \cdot (n\rho^i\mathbf{v}^i) = 0, \quad i = 1, \ldots, N-1, \tag{2}$$

where ρ^i is the mass of the ith component per unit volume of the liquid (mass concentration of the ith component), and $\mathbf{v}^i$ is the mass average velocity of the ith component. The densities and velocities of components and of mixture are related as follows:

$$\sum_{i=1}^{N} \rho^i = \rho, \qquad \sum_{i=1}^{N} \rho^i\mathbf{v}^i = \rho\mathbf{v}. \tag{3}$$

The transport of liquid through clayey liners is very slow and thus inertial forces and inertial interactions between liquid components are insignificant. Hence, the concept of strongly interacting constituents of liquid may be adopted [26]. Consequently, the balance of momentum for the considered system reduces to a single equation of linear momentum for the liquid mixture [11]:

$$\nabla \cdot \mathbf{T} + n\rho\mathbf{b} = \mathbf{R}, \tag{4}$$

where $\mathbf{T}$ is stress tensor in the liquid, $\mathbf{R}$ the interaction force between liquid and the porous matrix, and $\mathbf{b}$ the density of the external volume forces.

2.2. CONSTITUTIVE ASSUMPTIONS

The constitutive hypotheses needed to formulate the problem of contaminant transport concern the transport mechanisms and their possible evolution. The basic phenomena which control the transport of contaminants through low permeability soils are: flow of liquid induced by pressure gradient, diffusion of contaminants in the liquid phase driven by concentration gradient, and interaction of liquid and solid driven by various mechanisms, but usually related to concentration or its gradient, see [21, 22, 24]. In this paper, it is assumed that sorption has negligible effect and can be disregarded. Advective and diffusive transport are coupled through two mechanisms. First, a well established form of coupling occurs through dispersion, which although originally numerically insignificant for clays, depends on fluid velocity. The second type of coupling is typical of clays and is the focal point of this paper. It is postulated that during contamination, intrinsic permeability is a function of concentration. A characteristic increase in permeability of clay is observed when pore water is replaced by concentrated organic liquids or water solutions of salts [9, 16]. One of hypotheses used to explain it invokes a rearrangement of the pore structure of the clay fraction caused by the collapse of clay clusters due to chemically induced desorption of water (dehydration). At least two different scenarios of the influence of clay dehydration on permeability evolution are possible. One of them is based on the assumption that the dehydration causes significant changes of the volume of clayey material, leading to a macroscopic fracturing with the fracture size of the order of milli- or centimeters and a preferential flow of contaminants through the material [6]. Another model (following the findings of Fernandez and Quigley [9]) is based on a hypothesis that the volume changes of clay fraction cause the opening of micro-channels with the size of the order of micrometers and less, which control the permeability while no macro-channels are developed. Both scenarios are observed in soils depending on their fine fraction, mineralogy, water content, contaminant type, and testing techniques. This paper follows the latter idea incorporating a quantitative law of evolution of intrinsic permeability [14] to simulate the transport through clayey soils free of macro-cracks.

The specific assumptions of the model are as follows:

(1) Only one-dimensional transport is considered.

(2) The Darcy's law is formulated indirectly through the seepage force R between the liquid and the solid entering the linear momentum Equation (4). The force is proportional to the velocity of liquid with respect to solid:

$$R = \frac{\mu}{K}n^2v = \frac{\gamma}{\kappa}n^2v, \tag{5}$$

where K is intrinsic permeability of soil, μ is dynamic viscosity of fluid, κ ($= K\gamma/\mu$) is hydraulic conductivity, and γ ($= \rho g$) is unit weight of liquid. The value of coefficient of dynamic viscosity of liquid (mixture of water and contaminant) depends on the type of contaminant and is assumed as a polynomial function of concentration related to fluid density, c/ρ [27]:

$$\mu = \mu_w \frac{\rho}{\rho^w}\left[\mu_1\left(\frac{c}{\rho}\right)^3 + \mu_2\left(\frac{c}{\rho}\right)^2 + \mu_3\left(\frac{c}{\rho}\right) + \mu_4\right], \tag{6}$$

where c is concentration (mass of the contaminant per unit volume of the liquid), μ_w stands for viscosity of water while μ_1, μ_2, μ_3 and μ_4 are empirical constants.

(3) The phenomenological constitutive law for the evolution of intrinsic permeability is based on experimental data from the fixed wall, discharge controlled permeability tests conducted for Sarnia clay, permeated with dioxane with various concentration by Fernandez and Quigley [9]. These tests have shown an initial low sensitivity of permeability toward concentration, with a subsequent dramatic increase in permeability beginning around the mass fraction of contaminant of 0.7 (Figure 1). At the same time an evolution of pore space has been observed using mercury porosimetry, consisting in some changes in size and frequency of occurrence of dominant pore sizes. It is hypothesized that the permeation of clay with a relatively low dielectric constant organic causes dehydration of clay platelets and consequent shrinkage of clusters opening larger spaces between them. To simulate the permeability changes a micro-structural model of pore system conducting liquid has been proposed [14] as a series connection of larger and smaller channels formed by the dominant pores (Figure 2). The pores correspond to respectively unstressed and stressed contacts between clay domains of randomly oriented clusters of parallel platelets [18]. The size of the smaller channels located between parallel stressed interfaces is found to be critical for the flow discharge, as it results from the assumption of series connection of the pores. Intrinsic permeability of an elementary cell containing one such channel series is

$$K = \frac{B}{1/(\delta^v)^3 + 1/4(\delta^h)^3}, \tag{7}$$

where δ^h and δ^v stand for the sizes of smaller and larger channels, and B is a constant which depends on model parameters (size of elementary cell and tortuosity). Furthermore, it is assumed that chemical dehydration influences only the size of the smaller channels, δ^h, the following form of the evolution of this size is proposed:

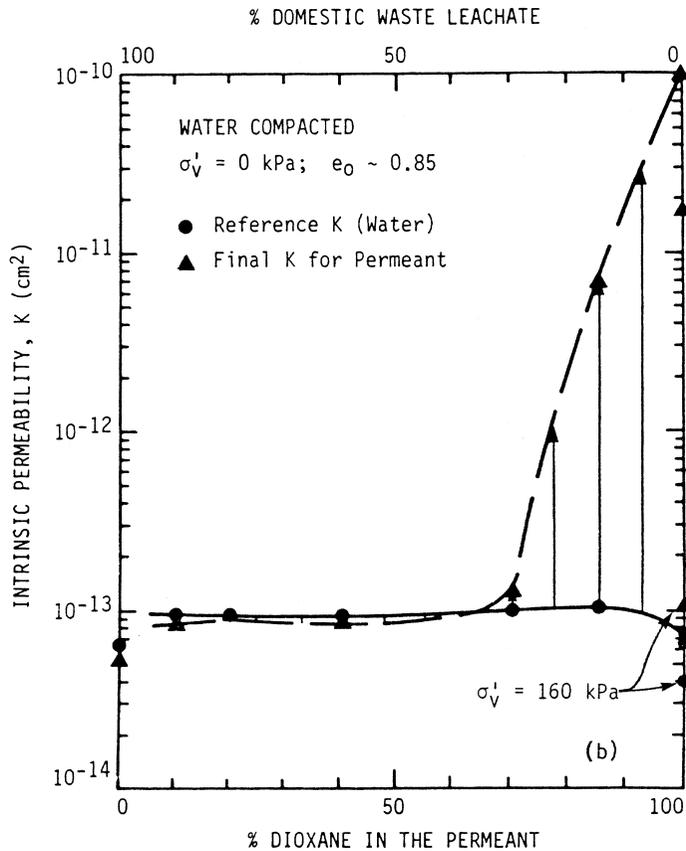$$\delta^h = \delta^{h0} + A(e^{\alpha c/\rho} - 1), \tag{8}$$

Figure 1. Intrinsic permeability of water compacted brown Sarnia clay permeated with leachate-dioxane mixtures. (All tests run originally with reference water, •, followed by permeants, △, varying from 100% leachate to 100% dioxane) – from [9]; σ'_{v0} is the effective vertical stress and e_0 the initial void ratio.

where A and α are constants to be determined from experimental data. It must be underlined that the above micro-mechanism is not the only one that can be visualized in chemically affected clays. Flocculation model, associated with particle rotation due to edge to face attraction has been seen to simulate well the measured permeability and pore system evolution [14]. The actual micro-structural changes seem to be a superposition of the above mechanisms.

(4) As a consequence of the assumption (3), porosity is unaffected by contamination. In fact, the smaller (variable) channels constitute a volume fraction about 50 times smaller than the larger ones, which remain constant.

(5) The liquid phase consists of water and a single contaminant miscible in water with density ρ^w and ρ^c, respectively. The volume of the liquid solution is assumed to be the sum of the volumes of the components taken separately at the same pressure
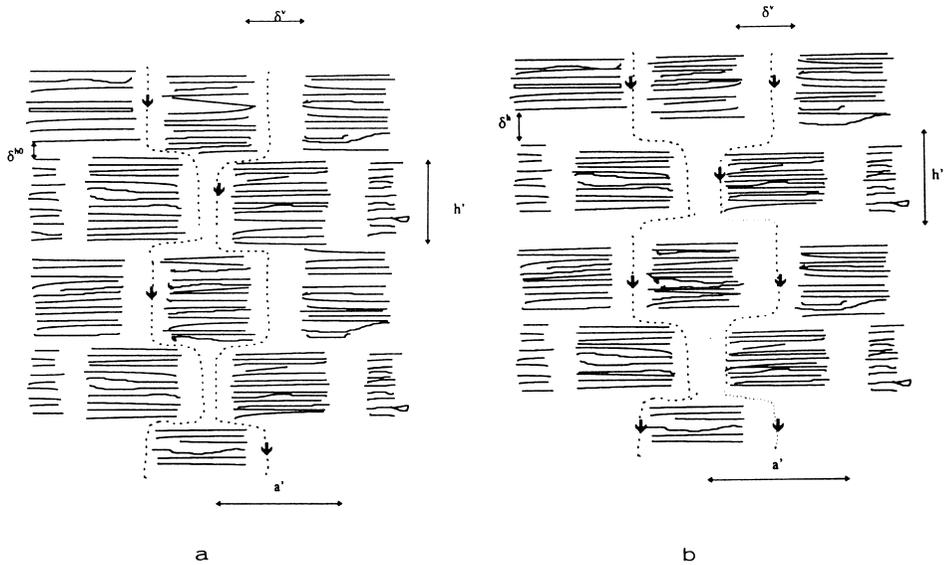
Figure 2. Pore size change model. (a) Schematic of the structure and flow of water permeated clay. Single lines correspond to clusters of parallely oriented platelets; (b) Structure and flow of dioxane permeated clay.

(perfect solution, see [20]). Hence, the relation between the density of liquid, ρ, and partial density of the contaminant c takes a form

$$\rho = \rho^w + c \left(1 - \frac{\rho^w}{\rho^c} \right). \tag{9}$$

(6) The liquid components do not react chemically with the solid or water.

(7) The deformations of solid skeleton and the changes of effective porosity of the soil during the transport are neglected. Since the volume of dehydrated water is extremely small, it is disregarded as a source in mass balance.

(8) The flux of mass of a contaminant, cv^c (v^c is the mass average pore velocity of the contaminant), is decomposed into advective, cv, and dispersive, $c(v^c - v)$, parts. The dispersive component of the flux is proportional to the gradient of the partial density of contaminant [3]:

$$c(v^c - v) = \tilde{D}\nabla c, \tag{10}$$

where $\tilde{D}$ is a coeffecient of dispersion. For one-dimensional case and isotropic porous medium, the coefficient $\tilde{D}$ may be represented as the sum of the effective coefficient of molecular diffusion D and of the term describing mechanical dispersion $d|v|$:

$$\tilde{D} = D + d|v|, \tag{11}$$

where d is a coefficient of longitudinal dispersion. It is assumed that the rearrangement of micro-structure, responsible for the evolution of permeability does not influence coefficients D and d, because they depend mainly on porosity, and characteristic

size of pores of the soil, which in the considered model are not strongly affected by the contaminant.

(9) The stress tensor in liquid is represented by a product of pore pressure, p, and porosity

$$T = -np. \tag{12}$$

2.3. GOVERNING EQUATIONS

The constitutive assumptions introduced in Section 2.2, and the balance Equations (1), (2) and (4), can be reduced to the following system of governing equations:

$$\bar{\rho}\frac{\partial c}{\partial t} + (\rho^w + c\bar{\rho})\frac{\partial v}{\partial x} + v\bar{\rho}\frac{\partial c}{\partial x} = 0, \tag{13}$$

$$\frac{\partial c}{\partial t} + c\frac{\partial v}{\partial x} + v\frac{\partial c}{\partial x} - (D + dv)\frac{\partial^2 c}{\partial x} - d\frac{\partial c}{\partial x}\frac{\partial v}{\partial x} = 0, \tag{14}$$

$$(\rho^w + c\bar{\rho})gK - K\frac{\partial p}{\partial x} - \mu n v = 0, \tag{15}$$

where

$$\bar{\rho} = 1 - \frac{\rho^w}{\rho^c}. \tag{16}$$

In this system the only dependent variables are c, v and p. D, d, g and n are constants and μ and K are known functions of c.

In general, Equations (13)–(15) constitute a system of coupled nonlinear partial differential equations which supplemented with initial and boundary conditions has to be solved numerically.

2.4. INITIAL AND BOUNDARY CONDITIONS

To investigate the transport of contaminant through clay with a chemically degradable permeability on engineering scale a one-dimensional diffusive–advective transport of a contaminant is considered through a finite layer. Two sets of simple initial and boundary conditions are analyzed. The initial concentration of the contaminant throughout the layer is zero. The pore pressure and concentration at the upper boundary, p_n, and c_n, are kept constant. At the lower boundary, the pressure, p_0, is assumed to be equal to zero while for concentration at the lower boundary two cases are considered. In the first case it is assumed that concentration is zero, while in the second case it is assumed that the gradient of concentration is equal to zero. The condition for constant concentration at the upper boundary corresponds to a continuous feeding by contaminant at the boundary. The two conditions at the lower boundary correspond

to a continuous perfect washing and lack of washing of the boundary, respectively (see [28]).

3. Numerical Simulation of Transport Through Liner

3.1. DISCRETIZATION

To discretize the governing partial differential equations, the implicit finite-difference method is used. Expansion of Equations (13)–(15) with finite-difference representations of derivatives leads to the following equations

$$\frac{\bar{\rho}}{\Delta t}(c_j^{n+1} - c_j^n) + \frac{1}{\Delta x}(\rho^w + \bar{\rho}c_j^{n+1})(v_{j+1}^{n+1} - v_j^{n+1}) +$$

$$+ \frac{\bar{\rho}}{2\Delta x}v_j^{n+1}(c_{j+1}^{n+1} - c_{j-1}^{n+1} - \xi c_{j-1}^{n+1} + 2\xi c_j^{n+1} - \xi c_{j+1}^{n+1}) = 0, \qquad (17)$$

$$\frac{1}{\Delta t}(c_j^{n+1} - c_j^n) + \frac{1}{\Delta x}c_j^{n+1}(v_{j+1}^{n+1} - v_j^{n+1}) +$$

$$+ \frac{1}{2\Delta x}v_j^{n+1}(c_{j+1}^{n+1} - c_{j-1}^{n+1} - \xi c_{j-1}^{n+1} + 2\xi c_j^{n+1} - \xi c_{j+1}^{n+1}) -$$

$$- \frac{(D + dv_j^{n+1})}{2(\Delta x)^2}(c_{j+1}^{n+1} - 2c_j^{n+1} + c_{j-1}^{n+1} + c_{j+1}^n - 2c_j^n + c_{j-1}^n) -$$

$$- \frac{d}{(\Delta x)^2}(c_j^{n+1} - c_{j-1}^{n+1})(v_{j+1}^{n+1} - v_j^{n+1}) = 0, \qquad (18)$$

$$(\rho^w + \bar{\rho}c_j^{n+1})gK - \frac{K}{\Delta x}(p_j^{n+1} - p_{j-1}^{n+1}) - \mu n v_j^{n+1} = 0, \qquad (19)$$

where Δx is the space grid size and Δt is the time step. The superscripts at the independent variables in Equations (17)–(19) refer to time index and the subscripts refer to the space index. The discretization involves using backward Euler method for the time derivatives, upwind differentiation for the first-order space derivatives and Crank–Nicolson scheme for the second-order space derivatives. Forward or backward differentiation is used for upwind differentiation depending on the direction of advective transport. In Equations (17) and (18), the concentration gradient is approximated using second-order upwind differentiation technique, see, e.g., [4, 19], whereby artificial diffusion (terms related to parameter ξ) is added to the advection term. This is required to satisfy the accuracy requirements in computation of fluid velocity, v^v [19].

The numerical solution of the above problem is obtained by setting up all three discretized governing equations at each internal point on the space grid. The initial condition is implemented by prescribing initial concentration at all the points

on the space grid. The boundary conditions are prescribed by fixing the values of concentration and pressure at the boundaries. Since concentration and pressure at the boundaries are defined by boundary conditions, while velocities at the boundaries are unknown, two additional equations are necessary, to determine the boundary values for the fluid velocity. The first one imposes the validity of the Darcy's law across the upper boundary. At the lower boundary, the extrapolation formula $v_2^{n+1} = v_1^{n+1} + \frac{1}{2}(v_2^{n+1} - v_0^{n+1})$ is used to relate the velocity at the boundary with velocities at the next two grid points. This gives a system of coupled algebraic equations to be solved for an equal number of unknowns – concentration, velocity, and pressure at each point on the grid. These equations can be expanded and readjusted so that the terms containing explicit unknowns (variables evaluated at the new time step) are on the left-hand side and the terms explicitly dependent only on the variables evaluated at the previous time step are on the right-hand side. This gives a set of simultaneous algebraic equations which for brevity are written in a matrix form as

$$\mathbf{A}\mathbf{y}^{n+1} = \mathbf{B}\mathbf{y}^n, \tag{20}$$

where $\mathbf{A}$ and $\mathbf{B}$ are the coefficient matrices depending on the unknowns, $\mathbf{y}^{n+1}$ is the vector of unknowns, and $\mathbf{y}^n$ is the vector of variables evaluated at the old time step. Due to the nonlinear nature of the considered partial differential equations the system of algebraic Equations (20) is also nonlinear. The solution to this system is obtained by using Newton–Raphson algorithm. This methodology involves an iterative evaluation of the incremental solution for each time step until the increments become sufficiently small as defined by the tolerance limits. The solution is considered satisfactory when the steady state is reached, i.e. when there is no significant change in the solution in successive time steps, or when an imposed maximum number of time step iterations is reached.

3.2. TEST OF THE NUMERICAL PROCEDURE

The above numerical procedure has first been tested against available analytical solution for a special case corresponding to constant pore fluid velocity and constant concentration at the boundaries (see, e.g., [17]) for which constant viscosity and permeability, and identical mass densities of water and contaminant were assumed. The pressure boundary condition at the upper boundary is 1 m of water, and the concentration of the contaminant with respect to water density amounts to 0.5. The pressure and concentration at the lower boundary are zero. The space grid size and the time step are equal to 0.033 m, and 0.2 yr, respectively. The values of intrinsic permeability, diffusion and dispersion coefficients are equal to 9.0×10^{-18} m^2, 0.01 m^2/yr, and 0.0875 mm.

The analytically and numerically obtained distributions of concentration for a few selected time instants are compared in Figure 3. The agreement of the results indicates that the applied method of discretization of the governing equations and
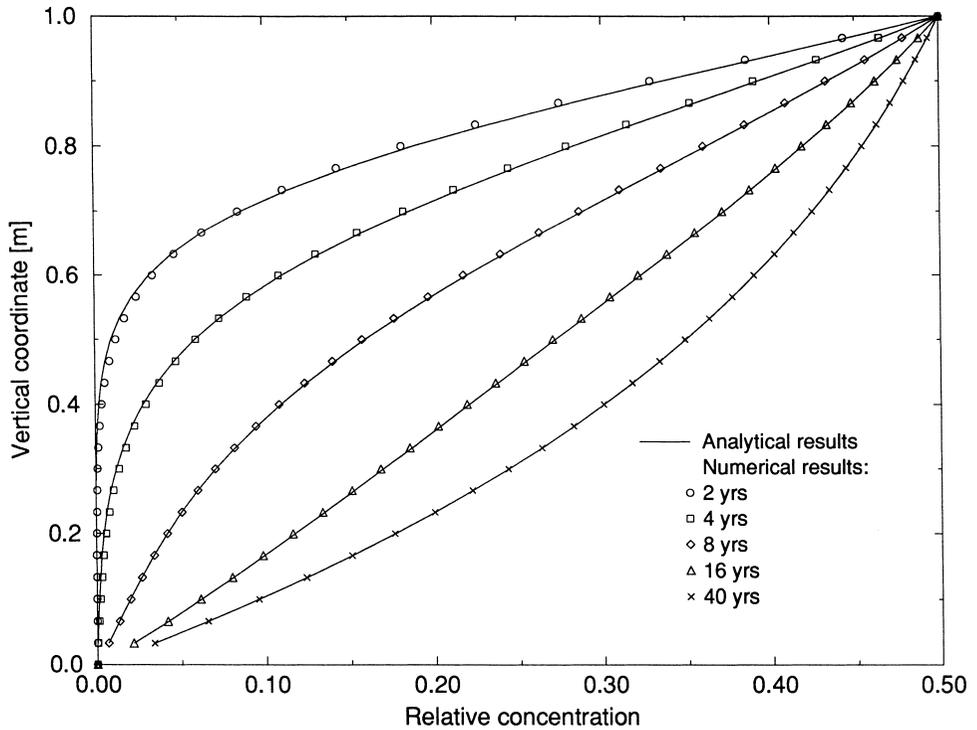
Figure 3. Distribution of relative concentration of contaminant (concentration divided by water density) across the layer. Comparison between an analytical and numerical solution for constant viscosity, constant permeability and identical water and contaminant densities.

in particular the effect of artificial diffusion introduced to assure the stability of numerical calculations for higher pore velocities do not imply significant deviation of the numerical solutions from the exact ones, even for long times and for transport dominated by diffusion.

3.3. RESULTS AND DISCUSSION

The transport of dioxane through an initially water saturated layer of Sarnia clay studied experimentally by Fernandez and Quigley [8, 9], is considered as an example. The thickness of the layer is taken as 1 m. The values of the material parameters used in the calculations are as given in Table I. The parameters which define the permeability evolution and viscosity of liquid mixture according to formulas (10) and (11) are determined using experimental data given by Fernandez and Quigley [8, 9]. The coefficients of diffusion and dispersion are typical ones for materials of soil liners.

To illustrate the dependence of constitutive functions on concentration of dioxane the variation of relative mass density, ρ/ρ^w, relative viscosity, μ/μ_{water}, of fluid, and relative intrinsic permeability of soil, K/K_{water}, as functions of mass fraction of the contaminant, c/ρ are shown in Figure 4. The dependence of intrinsic permeability on

Table I. Material parameters for the considered problem.

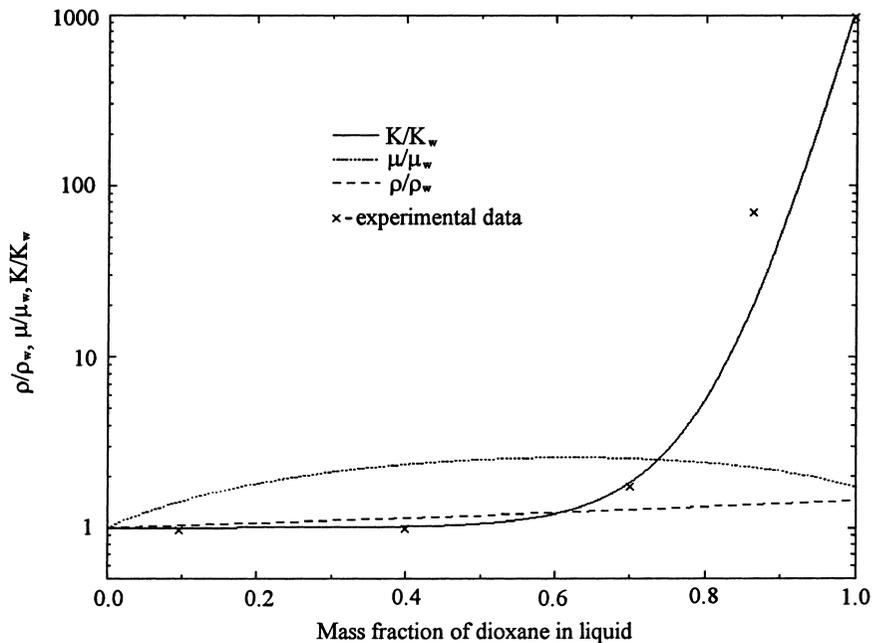| Material property	Value
g	0.976×10^{16} m/yr^2
ρ^w	1×10^3 kg/m^3
c	1.44×10^3 kg/m^3
μ_{water}	3.3×10^4 kg/m yr
D	0.01 m^2/yr
d	8.75×10^{-5} m
δ^v	3×10^{-6} m
δ^{h0}	6.7×10^{-8} m
B	7.576×10^3 m^{-1}
A	2.32×10^{-12}
α	12.52
n	0.3
μ_1	0.0
μ_2	-4.08
μ_3	4.28
μ_4	1.0

Figure 4. Variation of relative mass density, relative viscosity of fluid and relative intrinsic permeability of soil as functions of mass fraction of the contaminant in pore fluid following the proposed model. × – experimental data for Sarnia clay obtained by Fernandez and Quigley [8, 9].

Table II. Boundary conditions for concentration and pressure.

Case	Low concentration			High concentration		
1	$c/\rho^w = 0.5$	$t > 0$	$x = 1$ m	$c/\rho^w = 1.44$	$t > 0$	$x = 1$ m
	$c/\rho^w = 0$	$t > 0$	$x = 0$ m	$c/\rho^w = 0$	$t > 0$	$x = 0$ m
	$p = 3$ m^a	$t > 0$	$x = 1$ m	$p = 3$ m	$t > 0$	$x = 1$ m
	$p = 0$ m	$t > 0$	$x = 0$ m	$p = 0$ m	$t > 0$	$x = 0$ m
2	$c/\rho^w = 0.5$	$t > 0$	$x = 1$ m	$c/\rho^w = 1.44$	$t > 0$	$x = 1$ m
	$\partial c/\partial x = 0$	$t > 0$	$x = 0$ m	$\partial c/\partial x = 0$	$t > 0$	$x = 0$ m
	$p = 3$ m^a	$t > 0$	$x = 1$ m	$p = 3$ m	$t > 0$	$x = 1$ m
	$p = 0$ m	$t > 0$	$x = 0$ m	$p = 0$ m	$t > 0$	$x = 0$ m

^{a}Pressure in m of water head.

Table III. Initial conditions for concentration.

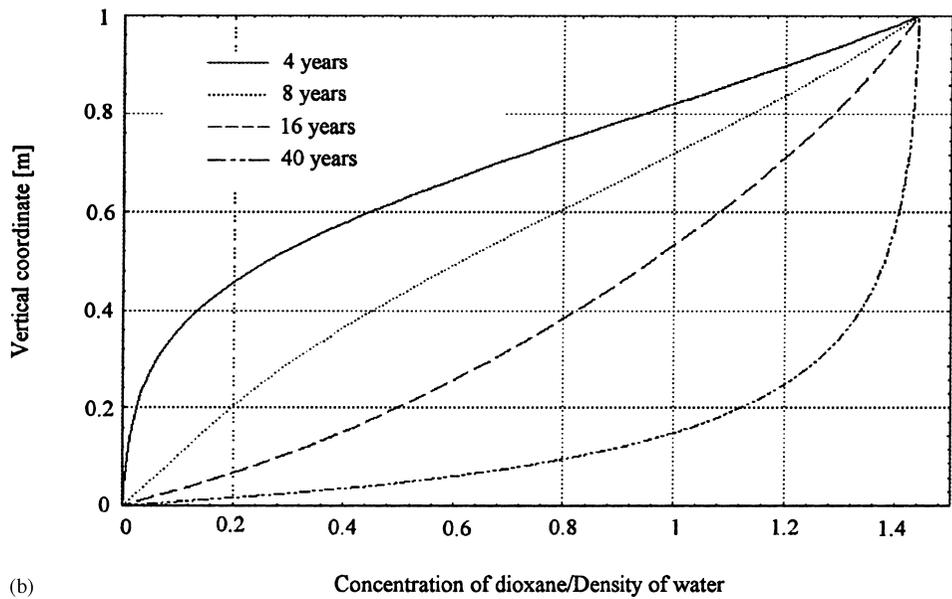| Low concentration			High concentration		
$c/\rho^w = 0$	$t = 0$	$0 \leqslant x < 1$ m	$c/\rho^w = 0$	$t = 0$	$0 \leqslant x < 1$ m
$c/\rho^w = 0.5$	$t = 0$	$x = 1$ m	$c/\rho^w = 1.44$	$t = 0$	$x = 1$ m

concentration approximating experimental data by Fernandez and Quigley [9] allows one to introduce rough distinction between regions of weak ($c/\rho < 0.7$) and strong ($c/\rho > 0.7$) sensitivity of intrinsic permeability to the contamination. To assess the role of this sensitivity for transport, the cases of low and high concentration of the contaminant at the upper boundary of the liner are considered separately. The complete set of boundary and initial conditions which corresponds to the constant concentration value at the upper boundary and the two cases of zero concentration and zero gradient of concentration of contaminant at the lower boundary are listed in Tables II and III, respectively.

Temporal evolution of the profiles of concentration, and liquid pressure throughout the layer subjected to low and high concentration at the upper boundary and for the two considered conditions at the lower boundary are shown in Figures 5–7. The distributions of concentration for the low concentration at the upper boundary and zero concentration at the lower boundary (Figure 5a) reaches a stationary state after about 40 yr. For comparison in Figure 5a prediction of steady state given by the analytical solution is shown. It is clear that the analytical solution (based on linear and uncoupled model) may give only a rough approximation of the solution which incorporates the variation of mass, viscosity of liquid and the couplings, although only slight changes in permeability occur for the low concentration case.

For the case of the high concentration at the upper boundary and zero concentration at the lower boundary, the evolution of distribution of concentration is given in Figure, 5b. Because of the strong nonlinearity of the equations (a slight variation of concentration induces a large change in permeability) the stationary state of concen-
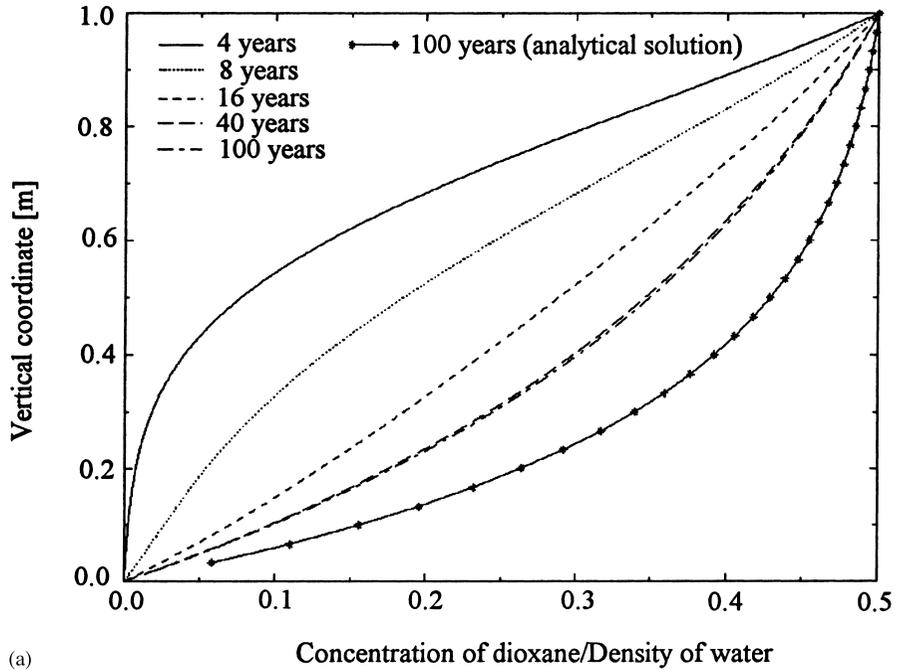
(a)

(b)

Figure 5. (a) Evolution of distribution of concentration of dioxane across the clay layer for zero concentration at the bottom boundary and low concentration imposed at the layer top. (b) Evolution of distribution of concentration of dioxane across the clay layer for zero concentration at the bottom boundary and high concentration imposed at the layer top.
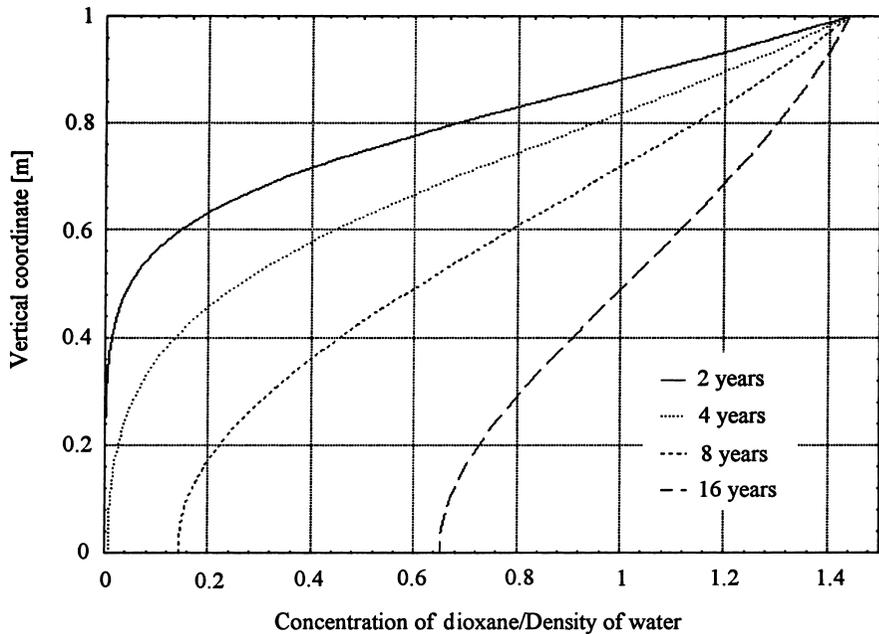
Figure 6. Evolution of distribution of concentration of dioxane across the clay layer for zero gradient of concentration at the bottom boundary and high concentration imposed at the layer top.

tration is not reached. High concentration of the contaminant spreads over almost the whole layer already at 40 yr as the result of increasing permeability. It is interesting to note that the velocity of fluid is only fifteen times higher than the initial value of velocity, which is much less than the increase of hydraulic conductivity in the major part of the layer (hydraulic conductivity increases about thousand times). There are two factors which limit the velocity evolution. One of them is the fact that for the one-dimensional problem with the above boundary conditions the layers more and less affected by the change in permeability are arranged in a series system. Since the lower part of the clay layer preserves low hydraulic conductivity, by the nature of the series system the advective mode of the transport is strongly attenuated. The second factor, which limits the growth of the advective velocity, is the zero concentration boundary condition at the washed lower boundary, which forces a drop of concentration and thus prevents an excessive change in permeability at the lower part.

The above attenuation of the increase of concentration and velocity is not observed in the case with zero gradient of concentration at the lower boundary. In such case the penetration of contaminant throughout the layer is significantly accelerated, see Figure 6, and finally the concentration reaches a homogeneous distribution. The maximum value of the pore fluid velocity in this case is about thousand times higher than the initial velocity, which practically means failure of the barrier. In the exam-
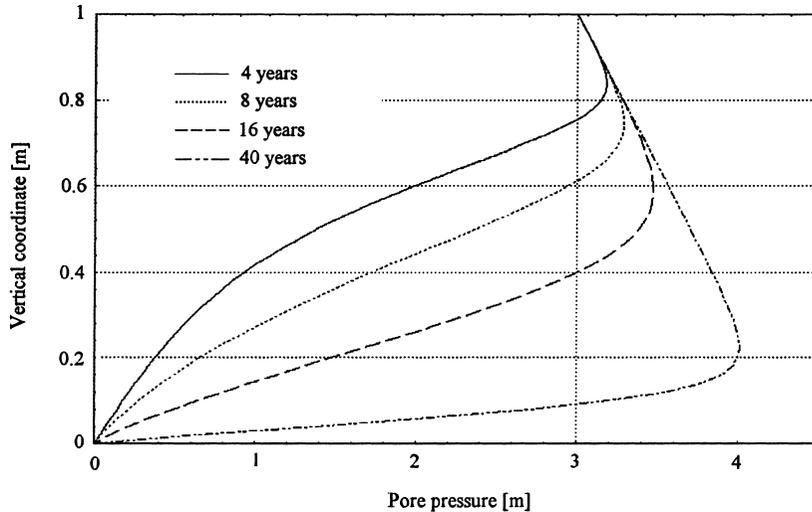
Figure 7. Evolution of distribution of pore pressure across the clay layer for zero concentration at the bottom boundary and high concentration of dioxane imposed at the layer top.

ples corresponding to high concentration of contaminant at the upper boundary, a significant deviation of pore pressure from the linear distribution is predicted. In the part of the layer affected by large changes of permeability, pore pressure raises substantially beyond the value prescribed at the upper boundary (see, e.g., results for case 1 in Figure 7). In fact, according to Equation (5), the interaction force between liquid and porous solid, which is the only source of dissipation of energy of fluid, is considerably smaller in the region of high concentration than in the rest of material. As a result, to maintain the equilibrium in the region of high concentration, the fluid pressure must increase.

To further investigate the consequences of the chemically driven variations in permeability at higher concentrations, let us examine the evolution of velocity of liquid with time (Figure 8). The mass averaged velocity of fluid is a primitive quantity in our model. To measure the volumetric flow across a unit area, we use the volume velocity of mass fluxes of water and of contaminant divided by the actual densities of water and contaminant, respectively. The temporal changes of volume velocity are the result of variation in fluid viscosity and intrinsic permeability of the porous material due to contamination. Initially, the enhancement of advective transport by diffusion takes place. Then, if the higher concentration at the upper boundary is applied, a breakthrough mechanism develops. The time of its occurrence seems to be very sensitive to the value of the imposed concentration at the top boundary and to the type of the lower boundary condition. For instance, a change in a lower boundary condition from zero concentration to zero gradient of concentration decreases the time of the breakthrough occurrence from about 43 to 21 yr (see Figure 8). On the other hand, a small difference in concentration at the influent boundary between 1.4
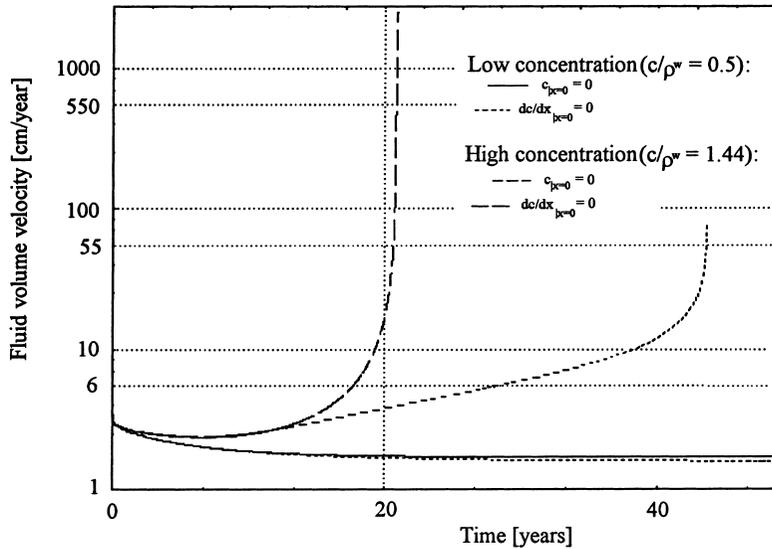
Figure 8. Evolution of distribution of fluid volume velocity of flow in time across the clay layer, for different concentrations of dioxane imposed at the layer top and different boundary conditions.

and 1.44 (the values of concentration are referred to the denisity of water) yields a shortening of the breakthrough time from about 54 to 43 yr.

Note also that, although the advective velocity in the considered case of the high concentration raises significantly (three orders of magnitude), the comparison of diffusion coefficient, D, and of parameter describing mechanical dispersion, $d|v|$, indicates that for both cases (low and high concentration) the mechanical dispersion still remains the secondary effect in the transport through clay liners. In the latter case, the mechanical dispersion rises to become about 17% of the coefficient of dispersion leading to an additional, but still minor coupling.

The above analysis is performed using a model which takes into account both advective and diffusive contributions to the development of contamination. Since most regulatory guidelines for construction of liners disregard the diffusive mechanism, it is instructive to compare the predictions of the coupled advective–diffusive model for zero concentration and zero gradient of concentration at the bottom boundary with the predictions of models in which advection is the only transport mechanism, see Figure 9. The comparison refers to the low concentration case, and two models of advective transport are considered. The first one totally disregards the changes in material parameters (density, viscosity, and permeability), and the other one neglects only the changes of density [14]. The advective models yield a significant time delay of the flux of contaminant at the lower boundary and/or a large deviation of the value of flux of contaminant at steady state, when compared to the coupled diffusion–advection model.
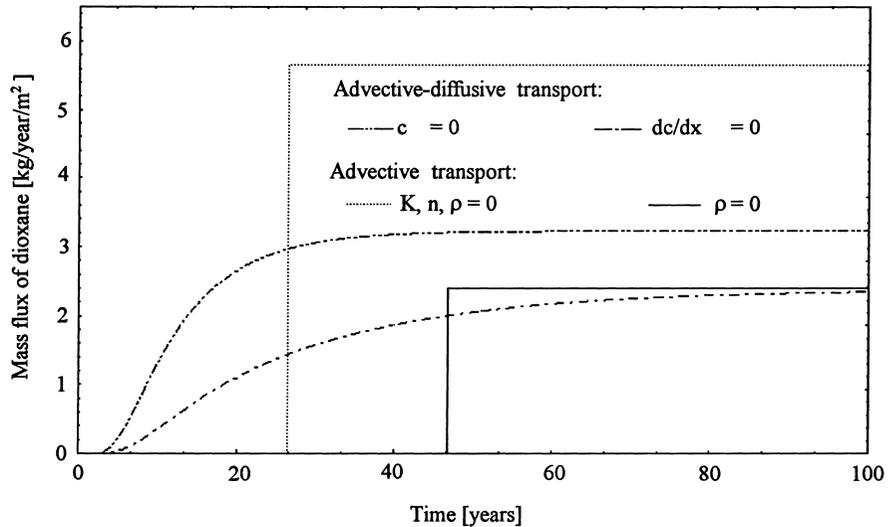
Figure 9. Mass flux of dioxane at the bottom boundary as a function of time. Low concentration of dioxane imposed at the layer top. Comparison of the simulations of the coupled diffusive–advective transport with: (1) purely advective transport with constant density, viscosity and permeability, and (2) purely advective transport with variable viscosity and permeability, and constant density of dioxane.

4. Conclusions

The results presented show the influence of two coupled phenomena: diffusion, and advection on the development of structural damage in clay barriers. In addition to the usual coupling through dispersion, which is initially insignificant in clays, the model includes the permeability sensitivity to organics at high concentration, following earlier findings for clays by Fernandez and Quigley [8] and Acar *et al.* [1]. For low and moderate concentration of contaminant at the top boundary, the diffusive component strongly influences transport. No large changes in permeability occur in the layer. Only an extremely high concentration imposed at the top boundary of the layer can cause a significant degradation of material impermeability throughout nearly the whole layer and a consequent domination of advective mechanism over diffusive mechanism of transport. It is shown that the propagation of the evolution of permeability and of the advective velocity is significantly slower if a low concentration occurs at the layer bottom. From the practical point of view this indicates the importance of a good leachate collection system, and an adverse effect of drain clogging. Thus, although in general diffusion contributes to an increase of the mass of the transported contaminant through liners, it may control the evolution of concentration and therefore of advective component of transport through chemically sensitive materials. The existence of positive feedback between transport of a contaminant and changes of permeability of a clay should be taken into consideration when the material of a liner is selected and a lining system is designed. In particular,

this refers to composite liners in which the upper layer, exposed to high concentration of contaminants, should possibly be made of a material insensitive to the chemistry of contaminants.

The results presented emphasize the need for the modeling of coupled phenomena in clay materials to determine phenomena which control transport and to ultimately allow to predict and possibly control the performance of clay liners. For a better approximation of the real life conditions, however, further studies of the coupled problems including sorption and reaction of contaminants with solid, interaction of components of liquid, and deformation of the solid material are recommended.

Acknowledgements

References

1. Acar, Y. B., Hamidon, A. B., Field, S. D. and Scott, L.: The effect of organic fluids on hydraulic conductivity of compacted kaolinite, In: A. I. Johnson, R. K. Frobel, N. J. Cavalli and C. B. Pettersson (eds), *Hydraulic Barriers in Soil and Rock*, ASTM STP 874, ASTM, 1985, pp. 171–187.
2. Allen, M. B., Herrera, I. and Pinder, G. F.: *Numerical Modeling in Science and Engineering*, Wiley, New York, 1988.
3. Bear, J.: *Dynamics of Fluids in Porous Media*, American Elsevier, New York, 1972.
4. Brooks, A. N. and Hughes, T. J. R.: Streamline upwind/Petrov–Galerkin formulations for convection dominated flows with particular emphasis on the incompressible Navier–Stokes equations, *Comput. Methods Appl. Mech. Engrg.* **32** (1982), 199–259.
5. Carnahan, C. L.: Simulation of reactive chemical transport in a varying thermal field with reaction-flow coupling, In: *Proc. 1st Int. Top Meet. High Level Radioactive Waste Manage*, Las Vegas, ASCE, 1990, pp. 143–147.
6. Daniel, D. E.: Clay liners, In: D. E. Daniel (ed.), *Geotechnical Practice for Waste Disposal*, Chapman and Hall, London, 1993, pp. 137–163.
7. DuChateau, P. and Zachmann, D.: *Applied Partial Differential Equations*, Harper and Row, New York, 1989.
8. Fernandez, F. and Quigley, R. M.: Hydraulic conductivity of natural clays permeated with simple liquid hydrocarbons, *Can. Geotech. J.* **22** (1985), 205–214.
9. Fernandez, F. and Quigley, R. M.: Viscosity and dielectric constant controls on the hydraulic conductivity of clayey Soils permeated with water-soluble organics, *Can. Geotech. J.* **25** (1988), 582–589.
10. Fernandez, F. and Quigley, R. M.: Controlling the destructive effects of clay – organic liquid interactions by application of effective stress, *Can. Geotech. J.* **28** (1991), 388–398.
11. Hassanizadeh, S. M.: Derivation of basic equations of mass transport in porous media, Part I – Macroscopic balance laws, *Adv. Water Resour.* **9** (1986), 196–206.
12. Hueckel, T.: Strain and contamination history dependence in chemo-plasticity of clays subjected to environmental loads, In: G. N. Pande and S. Pietruszczak (eds), *Numerical Models in Geomechanics*, NUMOG V, A. A. Balkema, Rotterdam, 1995, pp. 329–336.
13. Hueckel, T., Kaczmarek, M. and Zhang Q.: On the modeling of the role of stress in transport of contaminant in low clay content soils, In: H.Y. Fang and H. I. Inyang (eds), *Environmental Geotechnology* Vol. 1, Technomic Publ. Co., Lancaster, Pa, 1996, pp. 302–311.

14. Hueckel, T., Kaczmarek, M. and Caramuscio, P.: On the evolution of permeability of clay due to dehydration by organic contaminants, *Can. Geotech. J.* **34**, 1997, in print.

15. Jacobsen, J. C. and Carnahan, C. L.: *Coupled Processes in Semipermeable Media. II: Numerical Method and Results*, Lawrence Berkeley Laboratory, LBL-25619, 1990.

16. Mitchell, J. K. and Jaber, M.: Factors controlling the longterm preperties of clay liners, In: R. Bonaparte (ed.), *Waste Containment Systems: Construction, Regulation and Performance*, Geotechnical Special Publication No. 26, 1990, pp. ASCE, 84–105.

17. Mohamed, M. O., Yong, R. N., Tan, B. K., Farkas, A. and Curtis, L. W.: Geo-environmental assessment of a micaceous soil for its potential use as an engineered clay barrier, *Geotech. Testing J.* **17**(3) (1994), 291–304.

18. Murray, R. S. and Quirk, J. P.: Intrinsic failure and cracking of clay, *Soil Sci. Soc. Amer. J.* **54** (1990), 1179–1184.

19. Press, W. H., Teukolsky, S. A., Vellerling, W. T. and Flannery, B. P.: *Numerical Recipes in C – The Art of Scientific Computing*, 2nd edn, Cambridge University Press, Cambridge, 1992.

20. Prigogine, I. and Defay, R.: *Chemical Thermodynamics*, Longman and Green, London, 1954.

21. Quigley, R. M., Yanful, E. K. and Fernandez, F.: Ion transfer by diffusion through clayey bariers, In: R. D. Woods (ed), *Geotechnical Practice for Waste Disposal 87*, ASCE, 1987.

22. Rowe, R. K.: Pollutant transport through barriers, In: R. D. Woods (ed.), *Geotechnical Practice for Waste Disposal '87*, ASCE, 1987, pp. 159–181.

23. Rowe, R. K., Quigley, R. N. and Booker, J. R.: *Clayey Barrier Systems for Waste Disposal Facilities*, E. and F. N. Spon, London, 1995.

24. Shackelford, C. D.: Diffusion of contaminants through waste containment barriers, *Transport Res. Record* **1219** (1989), 169–182.

25. Steefel, C. I. and Lasaga, A.: Evolution of dissolution patterns, In: D. C. Melchior and R. L. Basset (eds), *Chemical Modeling in Aqueous Systems II*, Amer. Chem. Soc. Symposiums, Ser. 416, 1989, pp. 212–225.

26. Thomas, J. P.: The modeling of open mass continuum mixtures, *Int. J. Eng. Sci.* **11** (1991), 1451–1469.

27. Trompert, R. A., Verwer J. G. and Blom, J. G.: Computing brine transport in porous media with an adaptive-grid method, *Int. J. Num. Meth. Fluids* **16** (1993), 43–63.

28. van Genuchten, M. Th. and Parker, J. C.: Boundary conditions for displacement experiments through short laboratory soil columns, *Soil Sci. Soc. Am. J.* **48** (1984), 703–708.